

UKAEA-CCFE-PR(25)402

Hyun-Tae Kim, Eugenio Schuster, Fabien Jaulmes,
Geoffrey Cunningham, Gloria Falchetto, Hong-Sik
Yun, James Yang, Jeongwon Lee, Joelle Mailloux,
Oliver Bardsley, Peter de Vries, Runze Chen,

Takuma Wakatsuki, Xavier Litaudon, Yeongsun Lee,

Yong-Su Na, ITPA-Integrated Operating Scenario

MULTI-MACHINE VALIDATION OF PLASMA INITIATION MODELLING AND PROSPECTS FOR FUTURE DEVICES

Enquiries about copyright and reproduction should in the first instance be addressed to the UKAEA Publications Officer, Culham Science Centre, Building K1/0/83 Abingdon, Oxfordshire, OX14 3DB, UK. The United Kingdom Atomic Energy Authority is the copyright holder.

The contents of this document and all other UKAEA Preprints, Reports and Conference Papers are available to view online free at scientific-publications.ukaea.uk/

MULTI-MACHINE VALIDATION OF PLASMA INITIATION MODELLING AND PROSPECTS FOR FUTURE DEVICES

Hyun-Tae Kim, Eugenio Schuster, Fabien Jaulmes, Geoffrey Cunningham, Gloria Falchetto, Hong-Sik Yun, James Yang, Jeongwon Lee, Joelle Mailloux, Oliver Bardsley, Peter de Vries, Runze Chen, Takuma Wakatsuki, Xavier Litaudon, Yeongsun Lee, Yong-Su Na, ITPA-Integrated Operating Scenario group

MULTI-MACHINE VALIDATION OF PLASMA INITIATION MODELLING AND PROSPECTS FOR FUTURE DEVICES

Predicting plasma initiation using only hardware design and control room input data

¹Hyun-Tae Kim, ²Eugenio Schuster, ³Fabien Jaulmes, ¹Geoffrey Cunningham, ⁴Gloria Falchetto, ⁵Hong-Sik Yun, ⁶James Yang, ⁷Jeongwon Lee, ¹Joelle Mailloux, ¹Oliver Bardsley, ⁸Peter de Vries, ⁹Runze Chen, ¹⁰Takuma Wakatsuki, ⁴Xavier Litaudon, ⁵Yeongsun Lee, ⁵Yong-Su Na, and ITPA-Integrated Operating Scenario group

¹UKAEA (United Kingdom Atomic Energy Authority), Culham Campus, Abingdon, Oxfordshire, OX14 3DB, UK

²Department of Mechanical Engineering and Mechanics, Lehigh University, Bethlehem, PA, United States of America

³Institute of Plasma Physics of the CAS, Za Slovankou 1782/3, 182 00 Prague 8, Czech Republic

⁴IRFM, CEA F-13108, Saint-Paul-lez-Durance, France

⁵Department of Nuclear Engineering, Seoul National University, Seoul, Korea, Republic Of

⁶Princeton Plasma Physics Laboratory, Princeton University, Princeton, NJ, United States of America

⁷Korea Institute of Fusion Energy, Daejeon, Korea, Republic Of

⁸ITER Organization, Route de Vinon sur Verdon, 13067 St Paul Lez Durance, France

⁹Institute of Plasma Physics, Chinese Academy of Sciences, Hefei, China

¹⁰National Institutes for Quantum Science and Technology, Naka 311-0193, Japan

Abstract

Multi-machine validation of full electromagnetic plasma initiation modelling with DYON was carried out by the joint modelling of the International Tokamak Physics Activity (ITPA) - Integrating Operating Scenario (IOS) group. The following devices were included in the experiment database: VEST (spherical torus, copper coils, Stainless steel wall, $R/a=0.3\text{m}/0.2\text{m}$, $V_v=3.7\text{m}^3$), MAST-U (spherical torus, copper coils, C wall, $R/a=0.7\text{m}/0.5\text{m}$, $V_v=55\text{m}^3$), EAST (conventional tokamak, superconducting coils, metallic wall, $R/a=1.85\text{m}/0.5\text{m}$, $V_v=38\text{m}^3$), DIII-D (conventional tokamak, copper coils, C wall, $R/a=1.67\text{m}/0.65\text{m}$, $V_v=35\text{m}^3$), and KSTAR (conventional tokamak, superconducting coils, C wall, $R/a=1.8\text{m}/0.7\text{m}$, $V_v=55\text{m}^3$). Despite the different hardware features of the devices, the required operating spaces of the loop voltage induction and prefill gas pressure for inductive plasma initiation in each device were successfully reproduced by the predictive simulation with DYON using only the individual hardware design and the control room input data for each discharge. This successful validation across multiple machines demonstrates that the full electromagnetic DYON modelling can capture the essential physics of inductive plasma initiation. The simulation settings commonly employed for all modelling and the modifications necessary to account for the discrepancies between individual devices are reported. Predictions for ITER based on the multi-machine validation indicate that a wide range of prefill gas pressures exists for the Townsend breakdown and the plasma burn-through (0.01 ~ 1.5mPa). However, the risk of runaway electron generation must be assessed to confirm the operating space.

1. INTRODUCTION

The feasibility of plasma initiation is one of the most important aspects of designing a fusion device. The highest loop voltage throughout the plasma pulse is induced during the plasma initiation phase by fully charging and then rapidly decreasing the currents in the Central Solenoid (CS) and Poloidal Field (PF) coils. Therefore, the required specifications for the coils and power supplies depend on the feasibility of plasma initiation. In addition, the high loop voltage induces strong eddy currents that may hinder loop voltage induction in the vacuum centre and degrade the magnetic field null configuration. The toroidal electric conductivity of the vessel and surrounding supporting structures must also be considered in plasma initiation assessments.

In large superconducting tokamaks, such as ITER, EU-DEMO, and STEP, the inductive plasma initiation will be challenging due to the large vacuum space and the limited loop voltage [1]. To ensure the feasibility of plasma initiation during the design process and to optimise the operating scenario, it is important to develop and validate a reliable prediction tool that takes into account both the machine's hardware design and the control room input data i.e. coil currents and prefill gas pressure. Using the Electron Cyclotron (EC) wave for pre-ionisation and heating assistance facilitates the plasma initiation; however, EC modelling still requires further improvement and validation. In order to reduce the uncertainty in plasma initiation predictions involving integrated EC models, it is also important to confirm the validity of the inductive plasma initiation model alone.

DYON is a 0D plasma modelling code, dedicated to the plasma initiation phase [2]. It solves a system of the differential equations representing the global energy and particle balances of electrons, the main fuel and impurities in each charge state. DYON calculates both the parallel and perpendicular transport of energy and particles with respect to the magnetic field lines, which evolve from the fully open configuration to closed flux surfaces in the plasma initiation phase. The recycling of main fuels and the sputtering of impurities are calculated using the outward ion particle flux and plasma-wall interaction model [3]. The full circuit equations describing all toroidally conducting vessel structures, CS, and PF coils have been integrated into DYON [4]. This full electromagnetic feature enables the modelling of the vessel eddy currents and the calculation of the loop voltage in the plasma region with the CS and PF currents. Implementation of the full circuit equations enables the time evolution of the 2D poloidal magnetic flux map (i.e. ψ map) to be simulated in the vacuum space, with and without plasmas. This enables the Townsend breakdown to be evaluated along each field line and the plasma volume to be calculated in the burn-through phase.

The inductive plasma initiation prediction capability of the full electromagnetic DYON has been validated individually in MAST-U [5], VEST [6], EAST [7], DIII-D, and KSTAR. To confirm the generic validity of DYON in predicting the operation space, the ITPA-IOS group conducted a multimachine validation using a consistent simulation setup. This paper reports on the validation results and on predictive simulations for the inductive plasma initiation in ITER, based on the validated simulation setup.

2. EXPERIMENT DATABASE

One of the key objectives of the multi-machine validation is to test whether the predictive model can capture the essential physics without adjusting any free parameters for each device, which has very different hardware features such as aspect ratio, coil types, first wall material, ferromagnetic material, vacuum volume, plasma volume, toroidal magnetic field, and the effective connection length. Table 1 lists the devices in the experiment databases, and summarises their features. Since the aspect ratio (conventional tokamak or spherical torus) and the coil types (copper coils or superconducting coils) are different, the control room signals are also all different in each device. As an example, Figure 1 compares the time traces of central solenoid current, gas pressure, loop voltage, and plasma current in the five devices. In order to validate the generic capability of predicting individual discharges and thus the operating space in such different devices, five dedicated experiment databases were established by scanning the prefill gas pressure p_0 and the induced loop voltage V_{loop} .

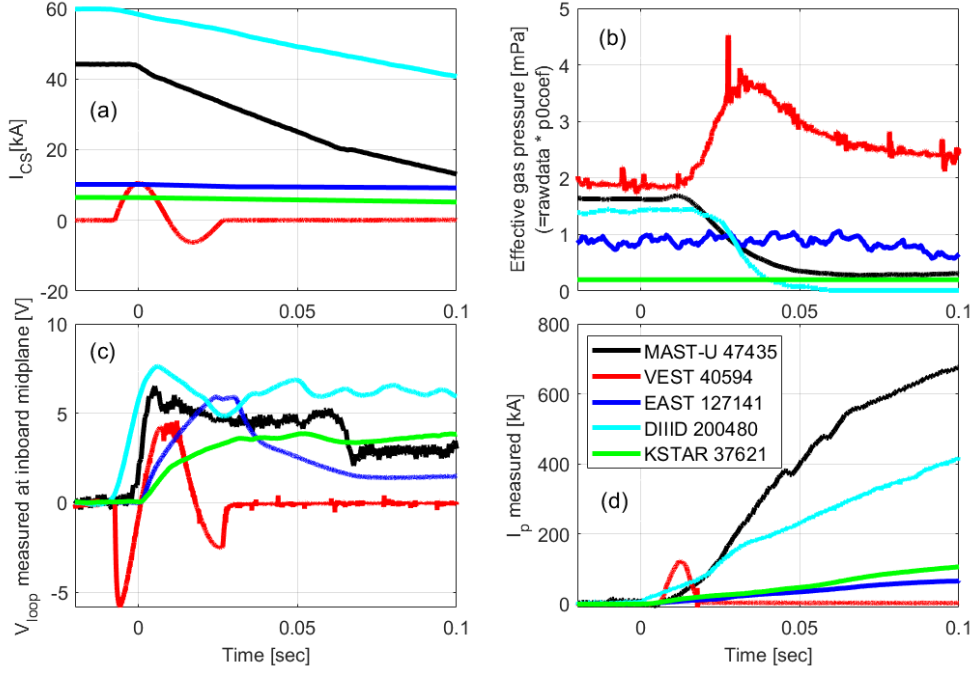


Figure 1(a) Central solenoid current (b) fuel gas pressure (c) measured loop voltage, and (d) the measured plasma current in MAST-U, VEST, EAST, DIII-D, and KSTAR

Figure 2 shows the operation spaces for inductive plasma initiation identified in the experiment databases. In the experiments, the discharges that achieved a sufficient increase in I_p (a few tens of kA) following successful Townsend breakdown and plasma burn-through were defined as successful plasma initiation. If a strong D_a signal was detected without a sufficient increase in I_p , the discharge was defined as plasma burn-through failure. If there was no or a very weak D_a signal detected with virtually zero I_p , the discharge was defined as Townsend breakdown failure. In all devices, it was commonly observed that the lower p_0 limit of the operation space was determined by the Townsend breakdown failure, while the upper p_0 limit and the lower V_{loop} limit are determined by the plasma burn-through failure. In the fusion community, the operation space for Townsend breakdown is often conventionally estimated using the Paschen curve, which is calculated with the effective connection length (L_f [m] = $0.25 \times a[m] \frac{B_\phi[T]}{B_\perp[T]}$) and the Townsend breakdown criteria ($V_{loop}[V/m] = 2\pi R[m] \times \frac{93.76 \times p_0[Pa]}{\ln(3.83 \times p_0[Pa] \times L_f[m])}$) [8]. The Paschen curves in Figure 2 were calculated with the parameters in Table 1 and the assumption of a good magnetic field null (i.e. 1mT of the stray magnetic field B_\perp). In all devices, the lower p_0 limits in Paschen curves are positioned far higher than the p_0 in the failed breakdown discharges in experiments. This suggests that L_f is not a valid measure to predict the operation space for Townsend breakdown, and a more complete calculation with modelling is necessary.

Table 1 Experiment databases for the multimachine validation of the operation space prediction of inductive plasma initiation (ST: Spherical Torus, CT: Conventional Tokamak).

| Device | Vacuum space geometry | Coils | First wall material | Ferromagnetic material | $V_v[m^3]$ | $V_p[m^3]$ | $B_t[T]$ | $L_f[m]$ |
|--------|-----------------------------|-----------------|---------------------|------------------------|------------|------------|----------|----------|
| MAST-U | ST ($R=0.7m$, $a=0.5m$) | Copper | C | N/A | 55 | 6 | 0.6 | 75 |
| EAST | CT ($R=1.85m$, $a=0.5m$) | Super Conductor | W + Mo | N/A | 38 | 7.5 | 2.5 | 311 |

| | | | | | | | | |
|--------|-----------------------------|--------------------|--------------------|----------------------------------------------------------|-----|-----|------|-----|
| DIII-D | CT (R=1.67m, a=0.65m) | Copper | C | N/A | 35 | 16 | 1.8 | 292 |
| KSTAR | CT (R=1.8m, a=0.7m) | Super Conductor | C | Incoloy 908 in the jacket of PF and TF coils | 55 | 5 | 1.8 | 315 |
| VEST | ST (R=0.3m, a=0.2m) | Copper | Stainless steel | N/A | 3.7 | 0.6 | 0.23 | 12 |

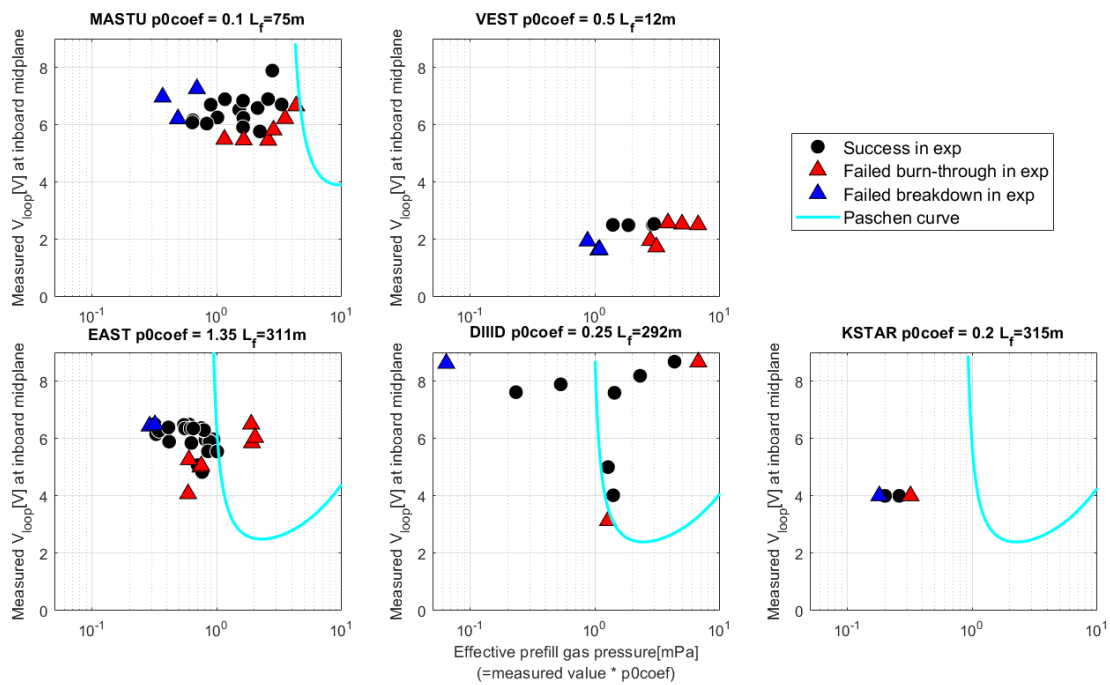


Figure 2 operation space for plasma initiation identified by scanning the loop voltage and the prefill gas pressure in MAST-U, VEST, EAST, DIII-D, and KSTAR experiments. Black circles: successful plasma initiation, Red triangles: failed burn-through, and Blue triangles: failed breakdown, and cyan lines: Paschen curves (the Paschen curve in VEST is positioned far higher than the experimental data, so not shown in the figure).

3. INPUT DATA AND SIMULATION SETUP

3.1. Input data – machine description, coil currents, and prefill gas pressure

In order for systematic validation of the full electromagnetic DYON on multiple machines, the same modelling strategy was employed for all devices. First, the electromagnetic response of the conducting structures was calibrated to represent the 3D nature (e.g. ports) in the 2D model. Figure 3 shows the active coils and the passive structures in the devices. By comparing the calculation of the induced loop voltage with the flux loop data, the resistivities of the passive structure elements were increased from the nominal values (e.g. 7.2e-7 [ohm*meter] for Stainless steel), which is valid only if the passive

structures are toroidally symmetric. Figure 4 shows the CS and PF currents used in the control room. Using the coil current input data and the calibrated machine description, the V_{loop} measured by the flux loop near the inboard mid-plane were successfully reproduced in the full electromagnetic DYON. This confirms the validity of the calibrated machine description.

The next step was to reproduce the plasma initiation phase in a reference discharge. The simulation results of plasma current, line radiation emission such as D_a , C-III, average T_e and n_e are then compared with the corresponding measured values. Examples of a reference discharge reproduction with DYON modelling are available in the previous publications (MAST-U [5] and EAST [7]). Based on the comparison with the experimental data, the prefill gas pressure value used in the modelling is corrected by multiplying it by a scaling factor (i.e. effective prefill gas pressure = p_0 coefficient \times measured fast ion gauge data) to account for errors, possibly arising from the distance between the plasma and the pressure diagnostic system, or/and the calibration error of the fast ion gauge. Finding the p_0 coefficient requires a reference discharge in existing devices, but this is less of a problem for predicting future devices. The prefill gas pressure can be easily adjusted during operation. It is important to predict whether there is a feasible gas pressure range that is wide enough at the given hardware and coil current scenarios. The p_0 coefficients reproducing a reference discharge are given in Table 2.

Table 2 Simulation setup to take into account the features of each device

| Device | Sputtering yield | Ferromagnetic modelling | p_0 coefficient |
|--------|------------------------------------------------|-------------------------|-------------------|
| MASTU | 0.1% initial O + C sputtering by D ions = 0.03 | N/A | 0.1 |
| EAST | 0.1% initial O | N/A | 1.35 |
| DIII-D | 0.1% initial O + C sputtering by D ions = 0.03 | N/A | 0.25 |
| KSTAR | 0.1% initial O + C sputtering by D ions = 0.03 | Done | 0.2 |
| VEST | 0.1% initial O | N/A | 0.5 |

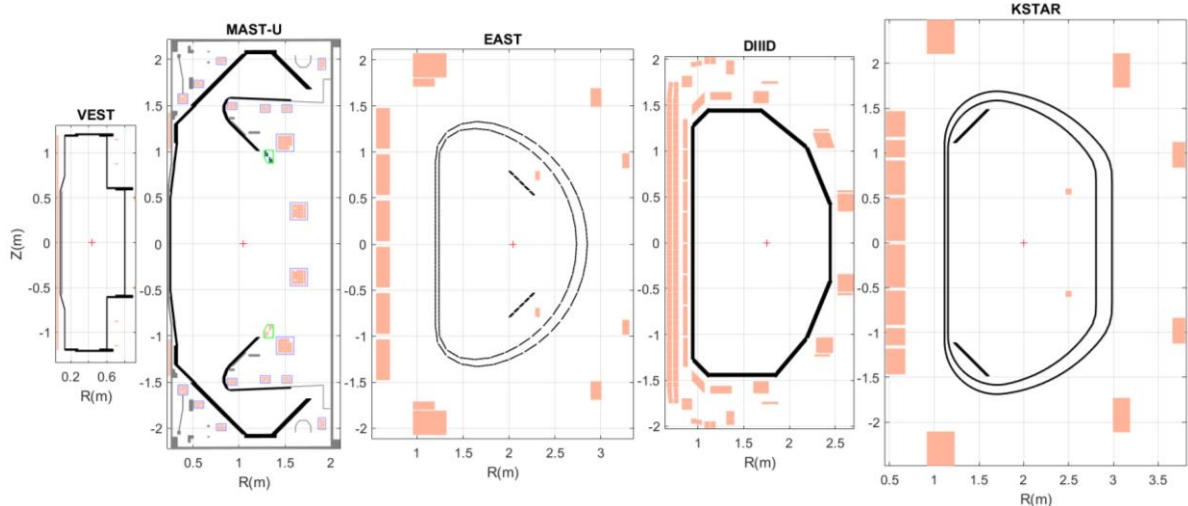


Figure 3 Description of CS and PF coils (in beige) and passive structures (in black, gray, or cyan) in the devices – VEST, MAST-U, EAST, DIII-D, and K-STAR

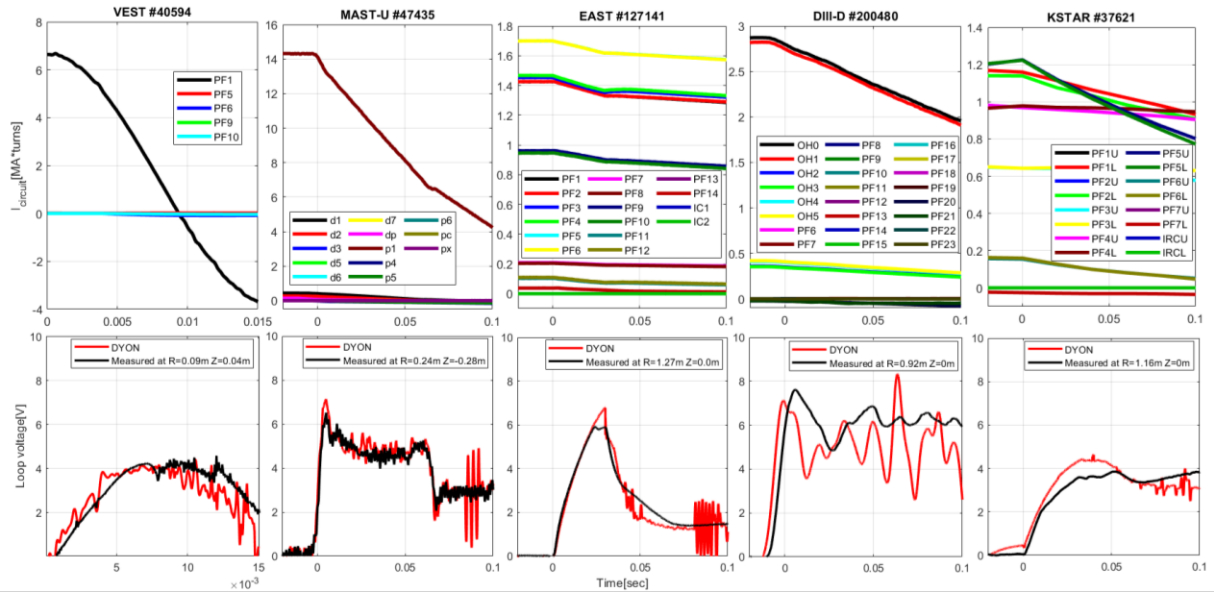


Figure 4 Coil currents and comparison of the loop voltages calculated (red) and the measured value (black) near the inboard mid-plane in each device – VEST, MAST-U, EAST, DIII-D, and K-STAR

3.2 Simulation setup

The choice of impurity sputtering models is subject to the first wall material in each device. The chemical sputtering from a metal first wall such as tungsten can be ignored. The ion temperature in the burn-through phase is less than 100eV, whereas the threshold incident ion energy required for physical sputtering at the tungsten wall is much higher than 100eV. In the devices with a metal first wall, the main impurity source is the impurities remaining in the prefill gas or lightly attached to the wall from the previous discharges, which could be instantly released once the Townsend breakdown occurs. On the other hand, the carbon first wall is chemically active, and the chemical sputtering by D ions and low-Z impurity ions (e.g. oxygen) [2] should be modelled. The wall conditions of discharges in the experiment databases were managed using between-shot glow discharge cleaning or wall treatments such as lithiumisation or boronisation. Therefore, it is reasonable to assume a low level of initial low-Z impurities in the prefill gas. Adjusting the initial low-Z impurity level in the modelling can help to better reproduce individual discharges. However, the initial impurity content is an uncertain parameter for future devices. To assess the generic prediction capability under the reasonable assumption of an initial low-Z impurity, the common initial oxygen of 0.1% in the prefill gas was used as the initial condition for modelling all devices.

Ferromagnetic material can distort the magnetic field configuration, degrading the null quality. KSTAR has a ferromagnetic material (Incoloy 908) in the jacket of the PF coils and all the Toroidal Field (TF) Coils [9]. To take into account the ferromagnetic effects, finite element method modelling of the nonlinear B - H curve of Incoloy 908 was performed, and the ferromagnetic 2D poloidal magnetic flux (i.e. ψ) was prescribed in the DYON modelling of KSTAR discharges. It was found that the prescribed ψ data were necessary for DYON to reproduce a successful plasma initiation in KSTAR #37621. Figure 5 compares the magnetic field configuration calculated by DYON with and without the ferromagnetic 2D poloidal magnetic flux. Without the ferromagnetic correction, the magnetic field null is not formed in the vacuum centre, and the breakdown fails in DYON. Such a ferromagnetic correction will be necessary for plasma initiation modelling in future devices if they contain ferromagnetic materials such as Incoloy 908. However, ITER does not have Incoloy 908 so the ferromagnetic effects were not modelled in the DYON prediction of ITER in this paper.

Apart from those described in Table 2, all the discharges in the multi-machine database are simulated with the same simulation setup, without any adjustment or tuning for individual devices or discharges.

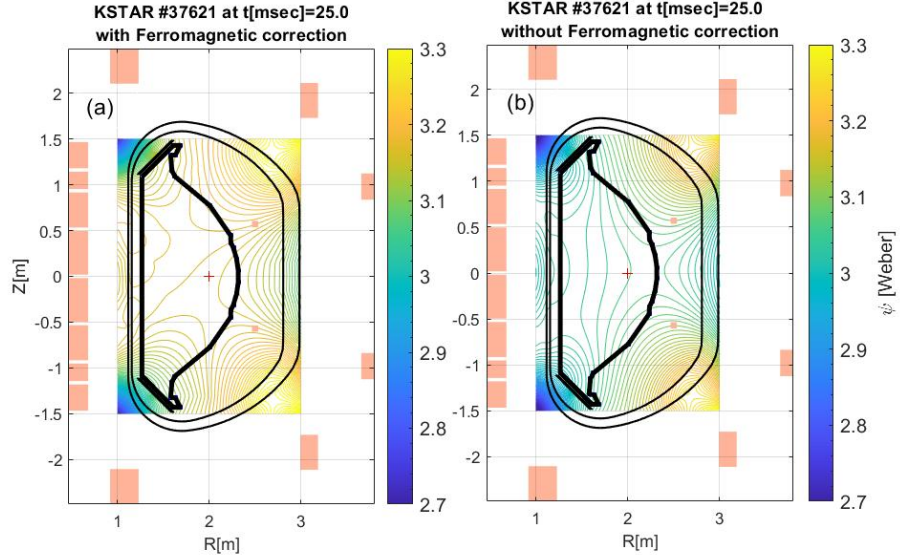


Figure 5 2D vacuum ψ map of KSTAR #37621 calculated by DYON (a) with and (b) without the ferromagnetic correction

4. MULTIMACHINE VALIDATION RESULTS

The experiment databases reveal common features. The lower and the upper limits of p_0 are determined by the Townsend breakdown failure and the plasma burn-through failure, respectively. The lower limit of V_{loop} is determined by the plasma burn-through failure. Using only the control room input data of each discharge (i.e. currents in the CS, PF and TF coils, p_0 , and the gas puffing rate) and with the simulation setup being the same for all devices apart from the parameters in Table 2, the full electromagnetic DYON correctly predicted the failed Townsend breakdown, failed plasma burn-through, and successful plasma initiation discharges for most discharges in all devices (see Figure 6). This successful demonstration across multiple machines proves the generic capability of predicting the operating space for inductive plasma initiation.

A couple of the failed burn-through discharges in MAST-U and VEST experiments were predicted to be successful in the modelling. The incorrectly predicted discharges are closely positioned to the lower V_{loop} limit of the operation space. The incorrect prediction should be due to the 0.1% initial oxygen in the prefill gas, which was identically defined in all discharges to assess the generic prediction capability. When increasing the initial oxygen to 2%, the failed burn-through discharges in experiments were correctly predicted in the modelling.

The lower p_0 limit predicted by the modelling is generally close to that observed in experiments. However, predictions of individual failed breakdown discharges are often inaccurate, requiring slightly lower or higher p_0 values for correct prediction. This may be because the Townsend breakdown assessment of individual open field lines in the present modelling does not capture some additional breakdown physics, although it is much more accurate than the conventional estimation with L_f . For example, the space charge during the breakdown phase could produce strong self-generated electric fields that can increase the convection losses of electrons by $E \times B$ drift [10] and cancel the externally induced V_{loop} and reduce the collisional ionisation rate along the magnetic field lines [11]. Also, when assessing the Townsend breakdown, DYON used $0.5 \times L_{open}$ (i.e. L_{open} is the calculated length of the individual open field lines). This factor 0.5 was adopted to estimate the actual travelling length of electrons, accounting for the arbitrary starting points of the seed electrons in open field lines. It has been reported that adjusting the factor helps to better reproduce the Townsend breakdown [12]. However, in order to take these additional physics into account in the modelling, some free parameters must be used

for each device or discharge. For the purpose of the multimachine validation in this paper, the additional breakdown physics models were not adopted.

The impact of a higher initial oxygen content in the prefill gas was investigated by testing the operation space prediction in EAST (see Figure 7), which is the database with the environment closest to ITER among the multimachine databases, i.e. it has superconducting coils with a metal wall in a conventional tokamak geometry. Up to 1% initial oxygen content in the prefill gas, there is no significant change in the predicted operation space. However, as the oxygen content increases beyond 1%, the operation space shrinks gradually from the upper p_0 boundary. The assessment indicates that the EAST operation space is best reproduced in predictive modelling with a low initial oxygen content (0 ~ 1%), which can be justified by the lithiumisation of the first wall performed before the experiments. Lithium has a low threshold energy of incident ions for physical sputtering, so the impact of the physical sputtering of lithium was tested [7]. The predicted operation space was not changed at all by the lithium physical sputtering, because of the low radiation power of lithium ions. The ITER operation plan involves boronising the first wall to reduce the initial oxygen level [13]. In the modelling with the boron physical sputtering, the predicted operation space remains almost unchanged. However, it should be noted that the test modelling with physical sputtering of lithium or boron assumed no initial content of either element. While it has been reported that initial lithium in the prefill gas has little impact, a few % of initial boron could reduce the operation space [7].

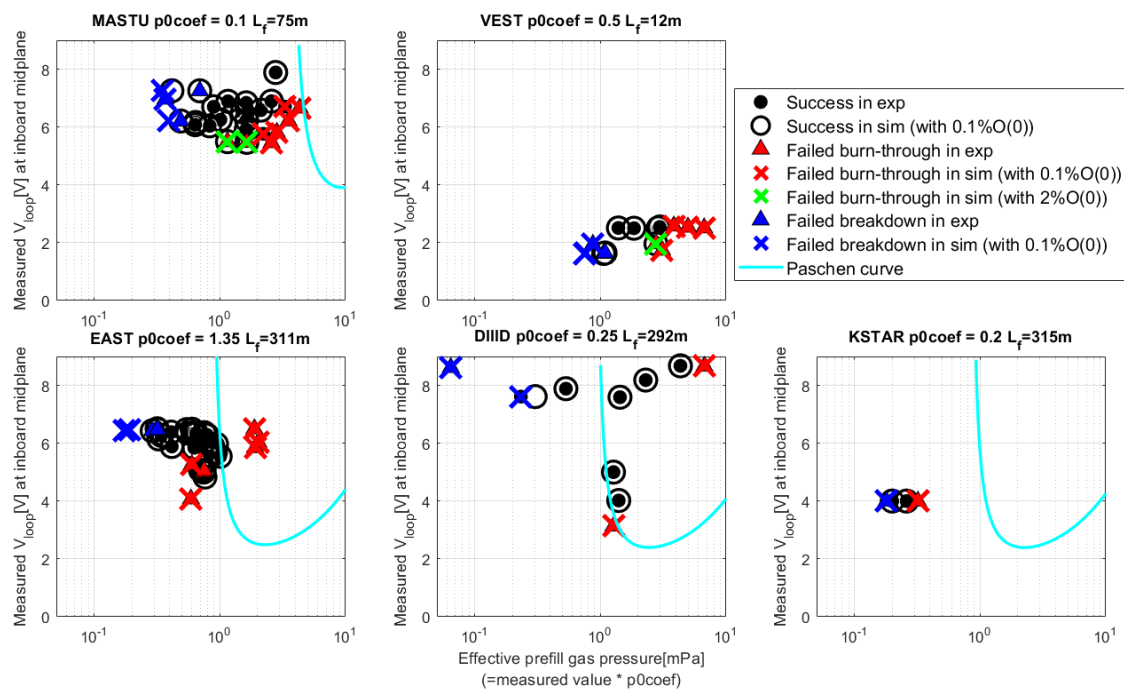


Figure 6 Operation space in the loop voltage at the inboard midplane and the effective prefill gas pressure for plasma initiation. The experimental data are indicated by filled black circles (successful plasma initiation), red triangles (failed burn-through), and blue triangles (failed breakdown). The corresponding predictive simulation results are indicated by open black circles (successful plasma initiation), red crosses (failed burn-through with the default simulation setup i.e. with 1% initial oxygen in the prefill gas, and blue crosses (failed breakdown). The green crosses indicate the failed burn-through in DYON with 2% initial oxygen. The cyan lines are Paschen curves calculated with L_f ($=0.25 * a \frac{B_t}{B_\perp}$).

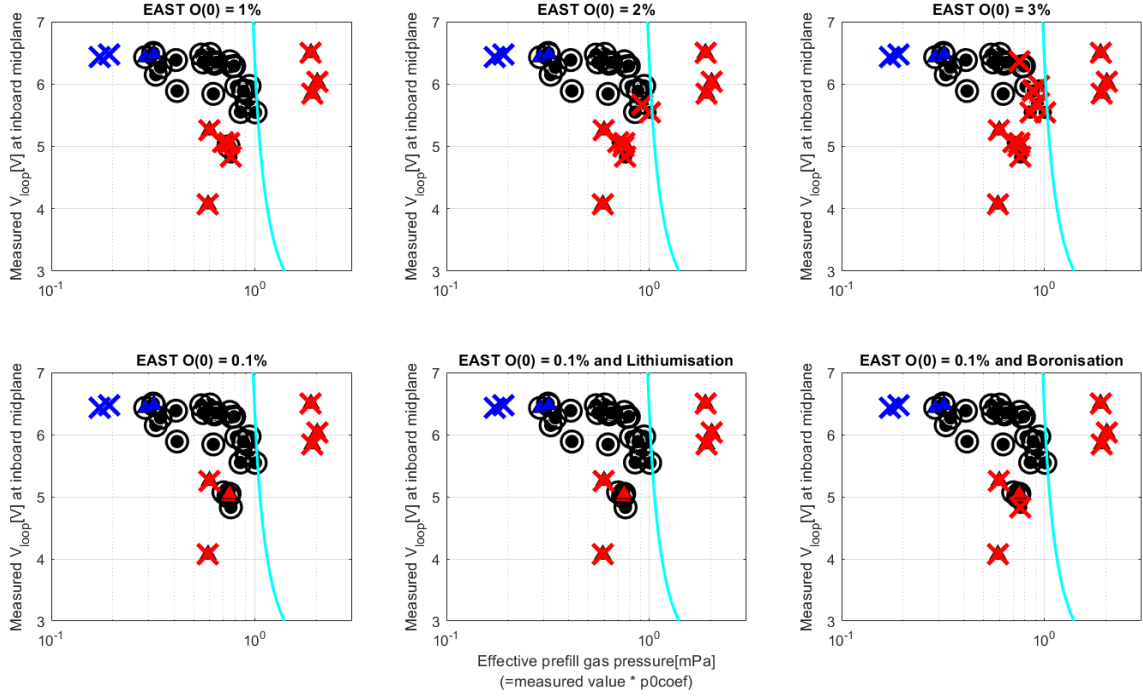


Figure 7 Operation spaces for plasma initiation with different initial oxygen and wall conditioning in EAST. The meaning of symbols are the same as Figure 3.

5. PREDICTION TO ITER

In the previous prediction, which did not take into account the full electromagnetic features, DYON predicted that the upper p_0 limit of plasma burn-through would be around 1mPa, and that the initial low-Z impurity content should be less than 1% for inductive plasma burn-through in ITER [14]. The same prediction results were obtained through modelling with SCENPLINT and BKD0 [15]. Predictive simulations of inductive plasma initiation in ITER have been performed again with the full electromagnetic DYON modelling. The machine description of ITER and the CS and PF currents (#105052) were obtained from the ITER Integrated Modelling and Analysis Suite (IMAS) [16]. Based on the EAST predictive modelling results, 0.1% initial oxygen and physical sputtering of boron were assumed. Figure 8 and Figure 9 (a)-(e) are the predictive simulation results at $p_0=1\text{mPa}$ in ITER, and Figure 9(f) indicates the p_0 range for inductive plasma initiation. DYON predicted that the upper p_0 limit is 1.5mPa, which is slightly higher than the previous prediction.

In the present devices, the completion of plasma burn-through typically takes less than 20-30ms at most (e.g. < 20ms in MAST-U [5]). However, in ITER, which has a much larger vacuum volume, the plasma current can only begin to ramp up at 750ms, once the pre-filled D gas has fully ionised. Until deuterium burn-through is completed, most of the electron energy from ohmic heating is radiated, and the electron temperature does not increase. Due to the high plasma resistance at the low electron temperature, the induced loop voltage is resistively dissipated, and drives large eddy currents (~ 1.3MA). Oxygen 5+ becomes dominant at 950ms, indicating that the plasma burn-through phase would take around 1 second to complete in ITER.

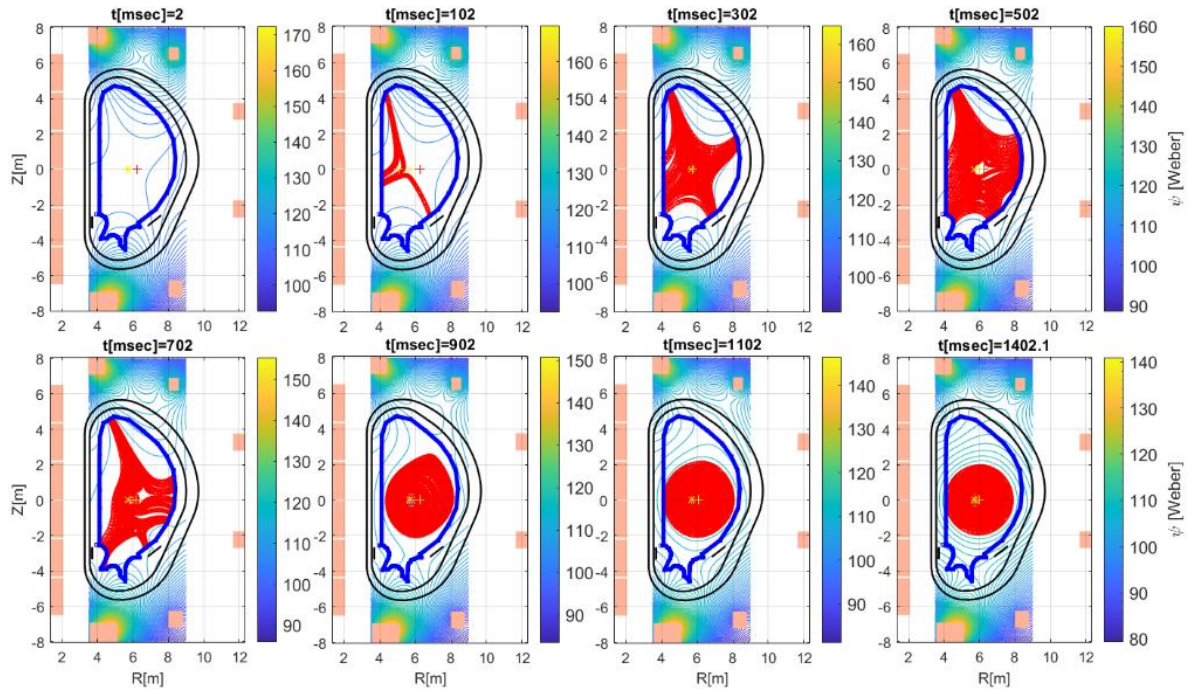


Figure 8 Example of ψ map evolution of ITER plasma initiation, simulated with full electromagnetic DYON with the operation scenario of 105052, 1mPa, 0.1% initial oxygen, and boron physical sputtering

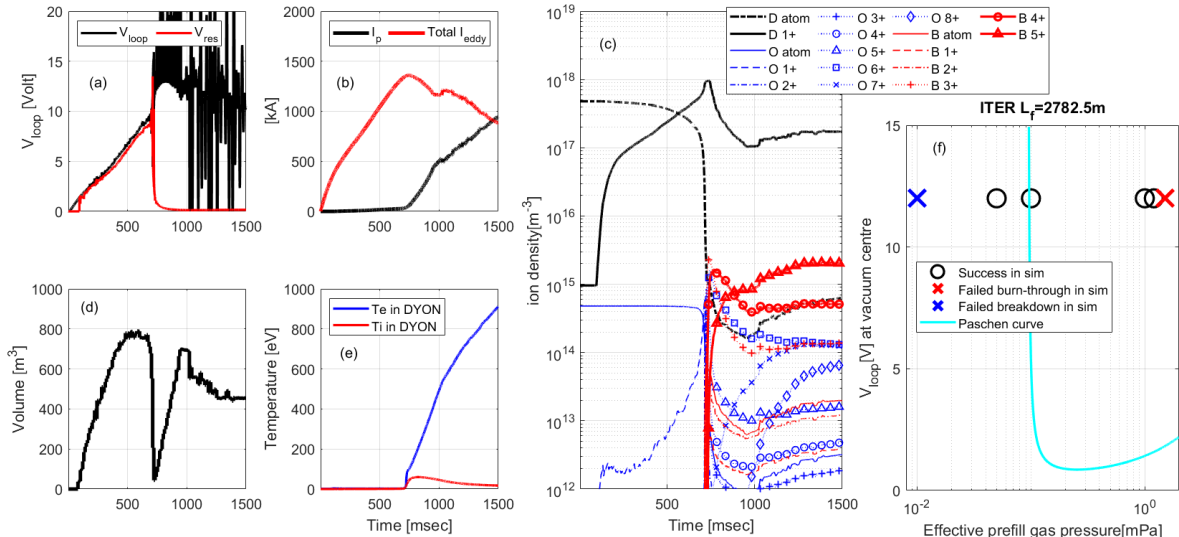


Figure 9 An example of DYON prediction of inductive plasma initiation in ITER ($p_0=1\text{mPa}$): (a)total induced loop voltage (black) and the resistive loop voltage(red), (b)plasma current (black) and total eddy current in the passive structures(red), (c)atom or ion densities of deuterium (black), oxygen(blue), and boron(red), (d)plasma volume, (e)temperatures of electrons(blue) and ions(red), and (f) operation space for inductive plasma initiation in ITER

Figure 9(c) shows that the ionisation of the D neutrals begins at 100ms. The V_{loop} is induced from 0 seconds and only reaches 2~3V at around 100ms. This suggests that the Townsend breakdown criteria are easily met at V_{loop} much lower than the ITER hardware limit (i.e. 12 V). The lower p_0 limit estimated by the Paschen curve is 0.1mPa, which is approximately one order of magnitude lower than those in the current devices. This is because the connection length in ITER is about an order of magnitude longer

than that in the existing devices. As observed in the multi-machine databases, the lower p_0 limit predicted by DYON modelling is also lower in ITER than the Paschen curve estimation. DYON predicted a lower p_0 limit of 0.01mPa for Townsend breakdown. This very low predicted p_0 limit could be verified by more complete breakdown modelling, such as BREAK [11].

Regarding the inductive operation space, the predictive modelling of plasma burn-through and Townsend breakdown indicates ITER has a wide range of p_0 for inductive plasma initiation (0.01mPa \sim 1.5mPa). However, it should be noted that we assumed effective boronisation of the first wall and a low level of initial impurity (0.1% initial oxygen in the prefill gas) in the ITER modelling. The initial oxygen level was scanned at 1mPa of p_0 , and DYON predicts that plasma burn-through fails with 5% initial oxygen in ITER. In other words, the upper limits of p_0 should be lower than 1.5mPa if there are significant initial impurities. Regarding the lower limit of p_0 , there is a risk of runaway electron generation during the plasma initiation phase. [17] states that runaway electrons can be produced for $p_0 < 1.7$ mPa. In such a case, there is no feasible operation space for inductive plasma initiation in ITER. However, more recent analyses have reported that the runaway electron generation is not simply a function of p_0 , and it must be assessed using proper modelling [1].

6. CONCLUSION

The excellent reproduction of the inductive operating space in the multi-machine databases demonstrates the full electromagnetic DYON's generic prediction capability and usefulness as a tool for assessing the hardware design of future devices and optimising operating scenarios. It also indicates the full electromagnetic DYON is ready to be used as a platform for testing further physics models, such as EC pre-ionisation and EC heating assistance. Predictions for ITER indicate that a wide range of p_0 values are possible for Townsend breakdown and plasma burn-through if initial impurities are minimised through effective boronisation of the first wall. However, uncertainties remain regarding runaway electron generation. A proper assessment using validated modelling of start-up runaway electrons is required to confirm the operation space for inductive plasma initiation in ITER.

ACKNOWLEDGEMENTS

This work has been carried out within the framework of the EUROfusion Consortium, funded by the European Union via the Euratom Research and Training Programme (Grant Agreement No. 101052200-EUROfusion) and from the EPSRC (Grant Number EP/W006839/1). This work was also supported in part by the U.S. Department of Energy Award DE-AC05-00OR22725. This research has also been supported by the Brain Korea 21 FOUR Program (No. 4199990314119). To obtain further information on the data and models underlying this paper please contact PublicationsManager@ukaea.uk*. Views and opinions expressed are however those of the author(s) only and do not necessarily reflect those of the European Union or the European Commission. Neither the European Union nor the European Commission can be held responsible for them.

REFERENCES

- [1] P. C. de Vries et al, "ITER breakdown and plasma initiation revisited," *Nuclear Fusion*, vol. 59, p. 096043, 2019.
- [2] Hyun-Tae Kim et al, "Enhancement of plasma burn-through simulation and validation in JET," *Nuclear Fusion*, vol. 52, p. 103016, 2012.
- [3] Hyun-Tae Kim et al, "Physics of plasma burn-through and DYON simulations for the JET ITER-like wall," *Plasma Physics and Controlled Fusion*, vol. 53, p. 083024, 2013.
- [4] Hyun-Tae Kim et al, "Development of full electromagnetic plasma burn-through model and validation in MAST," *Nuclear Fusion*, vol. 62, p. 126012, 2022.

- [5] Hyun-Tae Kim et al, "Validation of prediction capability of operating space for plasma initiation in MAST-U," *Nuclear Fusion*, vol. 64, p. 126010, 2024.
- [6] Hong-Sik Yun et al, "Improvement and validation of plasma initiation model for Versatile Experiment Spherical Torus," in *29th IAEA Fusion Energy Conference*, London, 2023.
- [7] Runze Chen et al, "Validation of DYON simulations and development of physical sputtering models for lithiation and boronisation in EAST," *Nuclear Fusion*, vol. 65, p. 076043, 2025.
- [8] ITER Physics Basis Expert Group on Disruptions, Plasma Control, and MHD, "Chapter 8: plasma operation and control," *Nuclear Fusion*, vol. 39, p. 2577, 1999.
- [9] Jayhyun Kim et al, "Stable plasma start-up in the KSTAR device under various discharge conditions," *Nuclear Fusion*, vol. 51, p. 083034, 2011.
- [10] M. Valovic , "Convective losses during current initiation in tokamaks," *Nuclear Fusion*, vol. 27, p. 599, 1987.
- [11] Min-Gu Yoo et al, "Evidence of a turbulent ExB mixing avalanche mechanism of gas breakdown in strongly magnetized systems," *Nature Communications*, vol. 9, p. 3523, 2018.
- [12] Ximan Li et al, "Development of plasma burn-through simulation code and validation in SUNIST-2 and EAST," *Nuclear Fusion*, vol. 65, p. 066017, 2025.
- [13] R. A. Pitt et al, "Plasma-wall interaction impact of the ITER re-baseline," *Nuclear Materials and Energy*, vol. 42, p. 101854, 2025.
- [14] Hyun-Tae Kim et al, "Plasma burn-through simulations using the DYON code and predictions for ITER," *Plasma Physics and Controlled Fusion*, vol. 55, p. 124032, 2013.
- [15] Hyun-Tae Kim et al, "Benchmarking of codes for plasma burn-through in tokamaks," *Nuclear Fusion*, vol. 60, p. 126049, 2020.
- [16] F. Imbeaux et al, "Design and first applications of the ITER integrated modelling and analysis suite," *Nuclear Fusion*, vol. 55, no. 12, p. 123006, 2015.
- [17] B. Lloyd et al, "ECRH-assisted start-up in ITER," *Plasma Physics and Controlled Fusion*, vol. 38, p. 1627, 1996.
- [18] B. Lloyd et al, "Low voltage ohmic and electron cyclotron heating assisted start-up in DIII-D," *Nuclear Fusion*, vol. 31, pp. 2031-53, 1991.